25th IMEKO TC4 International Symposium
23rd International Workshop on ADC and DAC Modelling and Testing
IMEKO TC-4 2022
Brescia, Italy /September 12-14, 2022

Design, metrological analysis and optimization of solenoid for homogenization of electromagnetic fields in biomedical experiments

Slavica Gajić[1], Platon Sovilj[2]

[1] *University of Banja Luka, Faculty of Electrical Engineering, Banja Luka, Bosnia and Herzegovina, slavica.gajic@etf.unibl.org*
[2] *Faculty of Technical Science, University of Novi Sad, Novi Sad, Serbia. e-mail: platon@uns.ac.rs*

Abstract **– In recent years, usage of electromagnetic field of static magnets in biomedical experiments is increased. It has been shown that extremely low-frequency (ELF) magnetic fields improve the impact of oncological therapy on cancer cells. Therefore, there is a huge need for ELF magnetic fields usage in biomedical experiments. In this paper, different designs and optimizations of solenoid for electromagnetic field homogenization along its axis, as well as in experimental volume, is compared. Using metrological analysis, the best design based on achieved homogenization of electromagnetic field and design complexity is selected. Also, a number of series expansions in 1st and 2nd kind of Elliptical integrals calculations is analysed in order to emphasize computer resources necessary for numerical modelling process.**

I. INTRODUCTION

In recent years, there is a great interest for the extremely low frequency (ELF) electromagnetic field in the scientific community, because of its influence on human life through different applications in the diagnosis and treatment of various diseases. Therefore, ELF fields are the subject of many researches, and there are many experiments performed *in vitro* on human and animal tissues, as well as *in vivo* on volunteers or with animals. In addition, the results of the experiments performed in a magnetic resonance (MR) scanner, and in a cyclotron magnet, indicate that strong static magnetic fields (SMFs) cause significant effects on the exposed body. It is well known that use of homogeneous, as well as inhomogeneous static magnetic fields initiate biomedical changes. There are evidences suggesting that SMFs have an effect on gene expression, calcium signaling, growth factor receptors, and cell cycle regulators [1]. Usage of those fields in therapy directly increases cytotoxic effects of the drugs in an *in vitro* cell growth assay. In the past two decades, analysis results suggest that SMFs can enhance the killing effect of antineoplastic drugs on cancer cells, indicating that SMFs may act synergistically with pharmacological treatment. Previous experiments have shown that combined treatment of 8.8 mT SMF with 10 mg/ml cisplatin (DDP) resulted in the inhibition of metabolic activity, a change in cell cycle distribution and serious damage to deoxyribonucleic acid (DNA) [2]. The application of SMF to human leukemia cells, combined with a mixture of chemotherapy drugs (5-fluorouracil, cisplatin, doxorubicin, and vincristine), enhanced the cytotoxic effects of the drugs in an in vitro cell growth assay1. Also, there is shown that SMF at 3.0 mT is able to sensitize cancer cells to Tumor necrosis factor a (TNF) -related apoptosis-inducing ligand (TRAIL) mediated apoptosis via the repression of Cdc2 and the subsequent downregulation of surviving (such as breast cancer cells), an anti-apoptotic protein demonstrating cell cycle-regulated expression. Effects of low strength SMF on Vascular Smooth Muscle Cells (VSMCs) biological performances, including proliferation, migration and adhesion are also described [3].

The state-of the-art technology where industrial electronics are called upon to play a key role in cancer treatment is described in [4]. Because of rapidly increasing use of ELFs fields in biomedical experiments, there are inevitable questions on the threshold levels of that fields, on the reversibility of arose effects, on how the effects depend on the field level, directions and homogeneity. To find answers on these all questions, researches require further experimenting. Preferably, that will be an exposure system designed for the purpose, which can provide scalable homogeneous ELF magnetic field with relatively strong peak value inside an experimental volume large enough to accommodate in vivo as well as in vitro experiments.

There are various methods in the literature that result in an increase in field uniformity inner the solenoid volume. One of them is a method [5] that uses copper plates and rings to obtain a modified solenoid with an experimental volume of 125 m, while the dimensions of the Helmholtz coil are adjusted for the homogenization of the magnetic field [6]. For the purpose of homogenizing relatively weak fields, a set of four circular coils arranged around the same axis with a larger number of coils on the inner

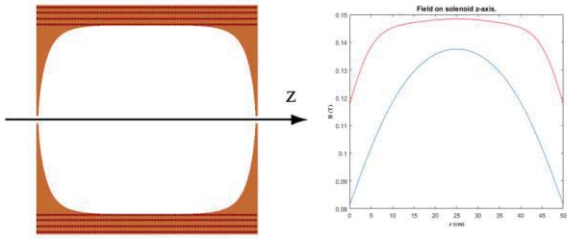

Fig. 1. Field flattening along solenoid axis. (a) The darker pattern emphasizes cross-section of a 50 cm long and 5 cm thick base solenoid. For ideal field flattening the additional wire windings form the shaped lid on each end of the solenoid [12]. (b) The magnetic induction along the solenoid axis for the base solenoid and solenoid with the additions (dimensions d = 6.5 cm and l = 5.5 cm), respectively.

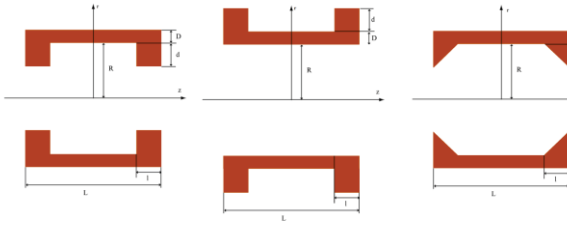

Fig. 2. Modified solenoid dimensions. The length and thickness of the basic solenoid are taken to be L and D, whereas the corresponding measures of the additional solenoids are l and d, respectively.

segments and a smaller radius of the outer segments is used [7]. Also, for this purpose square coils with sets of three, four and five further coils are proposed [8]. Design and optimization of a ring-pair permanent magnet array are proposed in [9] and compared with other proposed designs such as H-shaped magnet, C-shaped magnet, Halbach cylinder [10] and Aubert ring pair [11]. All of those designs are complex and difficult for hardware realization, so a simpler solution is required.

Main goal of this research is design and optimization of basic solenoid configuration to provide better homogeneity of electromagnetic field above solenoid axis, as well as in complete experimental volume. On this way, new solenoid design will be easier to realize and will be applicable in *in vitro* and *in vivo* biomedical experiments. Also, in this paper precision of numerical modeling process is tested. Obtained results are analyzed in order for provide information about dependency between used number of series expansion in 1st and 2nd kind of Elliptical integrals and calculation precision.

II. METHODS

A. Calculations

Magnetic induction along the axis B_z of a solenoid is derived using the Biot-Savart law by decomposing a solenoid into a set of very thin, i.e., single layer solenoids, and further into circular current loops, where R is inner radius, L is length, and D is thickness of solenoid, such as proposed in [12]. However, calculation of magnetic induction besides of solenoid axis is based on magnetic vector potential calculation in any point of 3D space and therefore is more complicated [13]. Because of the solenoid symmetry, cylindrical coordinate system is usually used for calculation process, where z, r and φ are its coordinates. Therefore, magnetic vector potential intensity doesn't depend of cylindrical coordinate φ, and calculation can be implemented in $\{r\text{-}O\text{-}z\}$ plane, for $\varphi = 0$. Then, the same concept of decomposing the solenoid into individual circular current loops proposed in [12] can be used. So, r-component and z-component of magnetic induction in any point in the 3D space inside the solenoid arises as the influence of only one winding is calculated as:

$$B_r = \frac{\mu_0 I}{2\pi} \frac{z}{r\sqrt{(R+r)^2+z^2}} \left[-K + \frac{R^2+r^2+z^2}{(R-r)^2+z^2} E \right], \quad (1)$$

$$B_z = \frac{\mu_0 I}{2\pi} \frac{1}{\sqrt{(R+r)^2+z^2}} \left[K + \frac{R^2-r^2-z^2}{(R-r)^2+z^2} E \right], \quad (2)$$

where R is radius of one current loop in solenoid corresponding to a wire segment, i.e. winding, with current I, and r and z are cylindrical coordinates of point in 3D space in which the magnetic induction is calculated ($\varphi = 0$). K and E are 1st and 2nd kind of Elliptic integrals:

$$K = \int_0^{\pi/2} \frac{dR}{\sqrt{1-k^2 \sin^2 R}}, \quad (3)$$

$$E = \int_0^{\pi/2} \sqrt{1-k^2 \sin^2 R}\, dR, \quad (4)$$

where k is:

$$k^2 = \frac{4Rr}{(R+r)^2+z^2}. \quad (5)$$

Integrals (3) and (4) expressed through series are:

$$K = \frac{\pi}{2}\left[1 + \left(\frac{1}{2}\right)^2 k^2 + \left(\frac{1\cdot 3}{2\cdot 4}\right)^2 k^4 + \cdots\right], \quad (6)$$

$$E = \frac{\pi}{2}\left[1 - \left(\frac{1}{2}\right)^2 k^2 - \left(\frac{1\cdot 3}{2\cdot 4}\right)^2 \frac{k^4}{3} - \cdots\right]. \quad (7)$$

It is easy to check that in points along solenoid axis ($r = 0$) equations (1) and (2) are reduced to:

$$B_r = 0, \quad B_z = \frac{\mu_0 I R^2}{2(R^2+z^2)^{3/2}}, \quad (8)$$

which represents an well-known term for the magnetic induction vector along the solenoid axis.

The derived formula quantitatively expresses the fact that magnetic induction along the axis of a solenoid is maximal in the solenoid's center and that it decreases towards each of solenoid's ends, for both of coordinates r and z. For example, the darker pattern in Fig. 1a emphasizes the cross-section of a 50 cm long and 5 cm thick solenoid with the inner radius of 17 cm (intended for testing in mice), whereas the corresponding magnetic field induction calculated using (1) - (2) and the current density of J = 2.7 A/mm^2 is given as the blue curve in Fig. 1b. In general, the described field can be flattened if the thickness of the solenoid is increased at its ends. Ideally, the additional windings shape of a modified solenoid which provides a constant value of magnetic induction along the axis, as well as inside 3D solenoid space [12] is illustrated witha brighter pattern in Fig. 1a. Additional rectangular shape wirewindings on each end of the solenoid, with dimensions d = 6.5 cm and l = 5.5 cm, results that field along the solenoid axis becomes more flat than forbasic solenoidandit is shown asred curve on Fig. 2b. Blue curve on Fig. 1.b corresponds of magnetic induction along the axis of basic solenoid.

The shape of a modified solenoid which provides ideal flattening inside 3D solenoid space would be quite difficult to wind. In addition, the volume that is required for biomedical experiments can be shorter than the solenoid length. Consequently, although it is desirable that the flat section of the field is as long as possible, it is not necessary that it covers complete length of the solenoid. Therefore, three simplified modifications of basic solenoid are provided for experimental tests and analysis of obtained results is presented.

The ideal additions with elaborate shape (see Fig. 1a) were replaced in three different ways in order to achieve the approximate elaborated design, i.e. by two simple rectangular shape solenoids in the following manner, at the inner ends of the base solenoid, at the external ends of the base solenoid and with two triangle shape solenoids inner base solenoid ends, as shown in Fig. 2. The length and thickness of the basic solenoid are defined with L and D, whereas the corresponding measures of the additional solenoids are l and d, respectively. In the case of triangle shape additions solenoids l and d arecathetus of triangle (see Fig 2).

In order to enable comparison of experimental test results obtained using different modified solenoids the same induction current density of 2.72 A/mm^2 is used in all cases. This value corresponds to the maximal current density of 3 A/mm^2 and the wire winding fill factor of 0.907. Therefore the fields obtained in all solenoids examples are the strongest available; for weaker fields, induction current should be adequately scaled. Besides, for purpose of testing process, inner radius of base solenoid R = 17 cm is chosen which suits to biomedical experimental volume intended for testing in mice.

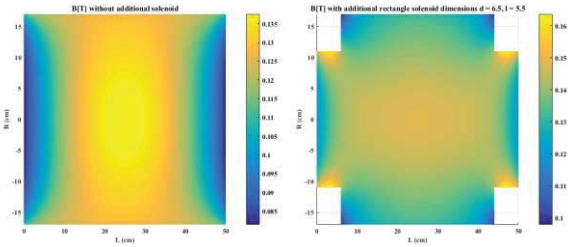

Fig. 3. Magnetic induction in 2D solenoid space for base solenoid and modified solenoid with additional dimensions d = 6.5 cm and l = 5.5 cm.

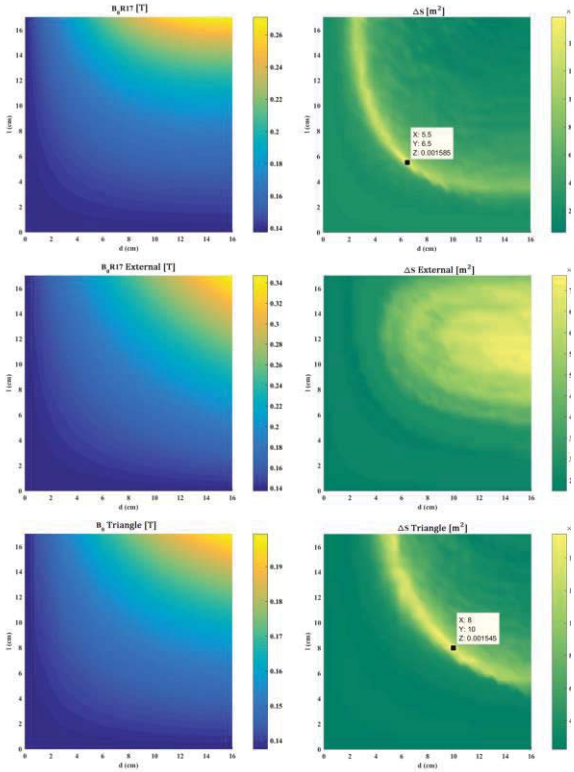

Fig. 4. Dependence of field level and flatness on size of additional solenoids(ΔB/B0 < 0.5 %).

III. RESULTS AND DISCUSSION

A. Analytical modeling

Proposed three simplified solenoid modifications of base solenoid are tested and (2) - (3) equations are used to study the influence of the modified solenoid dimensions on the strength and flatness of its field in 3D space. Because of solenoid symmetry, calculation is implemented in $\{r\text{-}O\text{-}z\}$ plane, for $\varphi = 0$.

With the increase of the additional solenoids' size, the shape of the field in inner solenoid space transforms from a surface with a maximum at $z = 0$, $r = 0$ to a surface with four local maximums. This transition is illustrated in Fig. 3 where first graph is without and second is with inner rectangle shape additions on solenoid ends with

dimensions d = 6.5 cm and l = 5.5 cm. Base solenoid is defined with L = 50 cm, D = 5 *cm*, R = 17 cm, as well as the similar results with others inner radius was obtained.

The two parameters chosen to quantitatively describe the strength and flatness of the field are B_0, the magnetic induction at z = 0, r = 0, and ΔS, the surface of the *{r-O-z}* plane segment along which the magnetic induction deviation is smaller than 0.5 % of B_0, i.e., along which $\Delta B/B_0$ < 0.5%. Field quality, described by these two parameters, depends on all five (*R, L, D, l, d*) dimensions that define the size of a modified solenoid. The influence of the additional solenoid size is investigated firstly, and the results for all of proposed additional solenoids are given in Fig. 4.

The field level, B_0, increases with the increase in d as well as in l, as can be seen in the left graphs in Fig. 4. The field flatness, ΔS, depends strongly on l as well as on d, and its large values are restricted to the narrow set of (*d, l*) pairs depicted with the bright area in the top and downright graphs in Fig. 4. As can be seen, the external additional solenoid doesn't provide good field flatness and value is 2 times lower compared to other additional solenoids. For additional rectangle shape solenoid dimensions pairs d = 6.5 cm, l = 5.5 cm there is maximum field flatness ΔS = 15.45 cm^2, as well as for triangle solenoid dimensions pairs d = 10 cm, l = 8 cm with ΔS = 15.85 cm^2. Due to symmetry, those values are valid for every angle φ, so these surfaces correspond to 97.07 cm^3 and 99.59 cm^3 volumes, respectively. Difference between those additional solenoids is in 0.4 cm^2 surface, i.e. 2.52 cm^3 volumes. Obtained result shows that the triangular additional solenoids ensure better field homogenization than additional solenoids rectangle shape. On the other hand, rectangle additional solenoid is much easier to wind. So, the solution should be chosen according to the required ratio of achieved performance and system complexity. The obtained qualitative dependence of B_0 and ΔS on the additional solenoid's length l as well as thickness d, is valid in general, regardless of the basic solenoid size, L and D.

For a biomedical experiment, it is preferred that conditions in the experimental volume are equal and that the ranges of available values of input parameters are as broad as possible. Based on the fact that additional solenoid rectangle shape is much easier to wind than triangle shape additional solenoid, those differences in surface/volume flatness can be disregard. So, other tests just on rectangle shape additional solenoid are evaluated. One more confirmation of field flatness is evaluated using standard deviation and variance of field without additional solenoids (base solenoid) and with additional solenoids rectangle shape with the best d = 6.5 cm and l = 5.5 cm parameters. Obtained results are given in Table 1 and it can be seen that modification of the solenoid provides better electromagnetic field homogenization.

B. Numerical modeling

In numerical modeling process, for integral calculation parameters K and E described with (6) and (7) are used. These parameters represent series of 1st and 2nd kind of Elliptic integrals, so calculation precision directly depends of used number of series expansion (n) in calculation process. Testing influence of the series expansion is evaluated in MATLAB, where n = 3, 4, 5, which is equivalent that K and E takes 3, 4, 5 members of the series, respectively. For testing of required execution time in those scenarios, Intel Core i7-3820 3.60 GHz processor with 64 GB of RAM and MATLAB function *cputime.m* are used. The results are given in Table 2. As can be seen, in case of basic solenoid, for n = 4 processor takes about 3.1 times more time for execution and for n = 5 it takes about 3.7 times more that time than for n = 3. For modified solenoid with rectangle shape additional solenoid with dimensions that provide the best field flatness, those times are about 3.3 and 4 times higher, respectively. Execution time extremely increases when n increases.

On the other hand, precision of numerical calculations in MATLAB doesn't so much degraded using just 3 series expansion n. This parameter doesn't influence on calculation precision of field intensity in solenoid center (z = 0, r = 0), there isminor influence on solenoid axis (r = 0), but withincreasing radius r the calculation error is also increased. Illustration of thosecalculation deviations is given on Fig. 5 and it represent differences between calculations with n = 3 and n = 4, i.e. n = 4 and n = 5, and n = 3 and n = 5, respectively, in all of *{r-O-z}* plane points, for φ = 0. Because of symmetry, those results are the same for all of $\varphi \in [0, 2\pi]$. Maximum difference values are 10^{-3} [mT] and 10^{-4} [mT] order, as shown in Table 3, where R = 17 cm, L = 50 cm and D = 5 cm. This speaks in favor that n = 3 is a sufficient number of series expansion used in the numerical calculation process based on eq. (6) and (7).

Table 1. Comparison of standard deviation and variance through {r-O-z} plane for basic and proposed solenoid.

Solenoid type	Stand. deviation	Variance
d = 0 cm and l = 0 cm	0.0036773	8.1998e-09
d = 6.5 cm and l = 5.5 cm	0.0021959	6.5419e-10

Table 2. Execution time for tested number of series expansions in 1st and 2nd kind of Elliptic integrals K and E that are used for integral calculation.

Execution time [s]	Number of series expansions (n)		
Solenoid type	3	4	5
d = 0 cm and l = 0 cm	125.33	391.47	467.58
d = 6.5 cm and l = 5.5 cm	15207	50004	60742

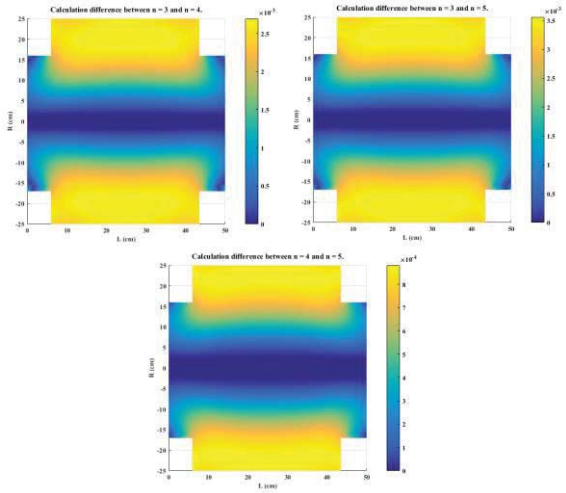

Fig. 5. Dependence of field level between different number of series expansions that are used for 1st and 2nd kind of Elliptic integrals calculation.

Table 3. Differences between calculations for different number of seriesexpansions in 1st and 2nd kind of Elliptic integrals K and E that are used for integral calculation.

Difference between:	n = 3 or 4	n = 4 or 5	n = 3 or 5
ΔB [mT]	$2.7 \cdot 10^{-3}$	$8.81 \cdot 10^{-4}$	$3.6 \cdot 10^{-3}$

IV. CONCLUSION

In this paper, solenoid modifications for purpose of its usage in biomedical experiments are proposed. Solenoid electromagnetic field homogenization along its axis, as well as in experimental volume is required. Three new solenoid designs are performed and their complexity and achieved performance are compared. It was concluded that triangle additional solenoids gives better field homogenization, while rectangle shape additional solenoids gives little weaker electromagnetic field homogenization, but this modification is easier to wind. Further, selected modified solenoid design for estimation of performed numerical calculations precision is used. It is obtained that number of series expansion, $n = 3$, has enough precision for numerical modeling. Experimental results show that solenoid modification designs provides more homogeneous field along its axis, as well as in all experimental volume compared with base solenoid.

REFERENCES

[1] T. Lin, et all, “A moderate static magnetic field enhances trail-induced apoptosis by the inhibition of cdc2 and subsequent downregulation of survivin in human breast carcinoma cells,” *Bioelectromagnetics*, vol. 35, no. 5, pp. 337–346, 2014.

[2] K. Zhang, et all, “Decreased p-glycoprotein is associated with the inhibitory effects of static magnetic fields and cisplatin on k562 cells,” *Bioelectromagnetics*, vol. 35, no. 6, pp. 437–443, 2014.

[3] Y. Li, L.-Q. Song, et al., “Low strength static magnetic field inhibits the proliferation, migration, and adhesion of human vascular smooth muscle cells in a restenosis model through mediating integrins β1-fak, ca 2+ signaling pathway,” *Annals of biomedical engineering*, vol. 40, no. 12, pp. 2611–2618, 2012.

[4] O. Lucia, H. Sarnago, et all, "Industrial Electronics for Biomedicine: A New Cancer Treatment Using Electroporation," in *IEEE Industrial Electronics Magazine*, vol. 13, no. 4, pp. 6-18, Dec. 2019.

[5] D. Bordelon, R. Goldstein, et all, “Modified solenoid coil that effciently produces high amplitude ac magnetic fields with enhanced uniformity for biomedical applications,” *IEEE transactions on magnetics,* vol. 48, no. 1, pp. 47–52, 2011.

[6] R. Beiranvand, “Effects of the winding cross-section shape on the magnetic field uniformity of the high field circular helmholtz coil systems,” *IEEE Transactions on Industrial Electronics*, vol. 64, no. 9, pp. 7120–7131, 2017.

[7] G. Gottardi, P. Mesirca, C. Agostini, D. Remondini, and F. Bersani, “A four coil exposure system (tetracoil) producing a highly uniform magnetic field,” Bioelectromagnetics: *Journal of the Bioelectromagnetics* Society, The Society for Physical Regulation in Biology and Medicine, The European Bioelectromagnetics Association, vol. 24, no. 2, pp. 125–133, 2003.

[8] R. Merritt, C. Purcell, and G. Stroink, “Uniform magnetic field produced by three, four, and five square coils,” *Review of Scientific Instruments,* vol. 54, no. 7, pp. 879–882, 1983.

[9] Z. H. Ren, W. C. Mu and S. Y. Huang, "Design and Optimization of a Ring-Pair Permanent Magnet Array for Head Imaging in a Low-Field Portable MRI System," in *IEEE Transactions on Magnetics,* vol. 55, no. 1, pp. 1-8, Jan. 2019, Art no. 5100108.

[10] K. Halbach, “Design of permanent multipole magnets with oriented rare Earth cobalt material,” *Nucl. Instrum. Methods*, vol. 169, no. 1, pp. 1–10, 1980.

[11] G. Aubert, “Permanent magnet for nuclear magnetic resonance imaging equipment,” U.S. Patent 5332971, Jul. 26, 1994.

[12] Jasna Ristic-Djurovic, et all, „Desing and Optimization of electromagnets for Biomedical Experiments With Static Magnetic and ELF Electromagnetic Fields”, *IEEE Trans. on Industrial Electronics*, ISSN: 0278-0046, vol. 65, no. 6, pp. 4991-5000, June 2018, (doi: 10.1109/TIE.2017.2772158)

[13] A. Djordjevic, Osnovielektrotehnike, 3. deo, Elektromagnetizam. Akademska Misao, 2007.